Experimental and numerical study on HDPE/SWCNT nanocomposite elastic properties considering the processing techniques effect

R. T. Tebeta[1] · A. M. Fattahi[1] · N. A. Ahmed[1]

Abstract

The aim of this study is to evaluate the elastic properties of high-density polyethylene (HDPE) using single-walled carbon nanotubes (SWCNTs) reinforcements with experimental and Finite element method (FEM) considering two different processing techniques effect. SWCNT nanoparticles were used to strengthen the HDPE matrix at the weight fractions (wt%) of 0, 0.2, 0.4, 0.6, 0.8, and 1 and the resulting nanocomposites were processed using injection and compression moulding. From each processing method, the HDPE/SWCNTs nanocomposites tensile test specimen were prepared and tested for the elastic properties. Experimental results showed that the addition of SWCNT nanoparticles for each weight fractions and both processing methods enhanced the elastic properties of HDPE. Finally, the numerical simulations were conducted using FEM for the prediction of the elastic modulus of HDPE/SWCNT nanocomposites for both processing methods. Whereby the representative volume element (RVE) model was presented with an interfacial phase region separating the load transfer between the SWCNT and HDPE with the properties obtained from the atomic modelling results. The numerical FEM elastic modulus results were found to correlate with the experimental results.

1 Introduction

The main reason why composites/nanocomposites materials are developed is that there is no material on its own that can be found to possess a uniform structural property with all features required for certain industrial application. The most interesting aspect of the introduction of composite materials is their ability to composed of two or more properties that are specifically for certain engineering application (Safaei et al. 2018, 2019a, b, c; Yang et al. 2020; Fattahi et al. 2019a, b; Qin et al. 2017; Liu et al. 2020). According to Crawford (1998), polymeric composites materials are commonly developed and used.

Developing a new polymer of distinct properties has been influenced by its diverse application. The quality of such polymeric composite is, however, dependent on the processing techniques and the precision with which it can be manufactured (Ho et al. 2012). Reinforcing polymer with nanoparticles has been an attracting field of

nanotechnology and for most polymer manufacturing companies (Huang et al. 2003). Nanotechnology is the field of study that deals with developing device, materials, or processing structures with at least one dimension measured from 1 to 100 nm (nanometres) (Thakur et al. 2012; Ullah 2012). According to Fattahi et al. (Fattahi et al. 2018), reinforcing polymers with carbon nanotubes (CNTs) have become popular and applied in many fields such as automotive, wind turbine, aerospace, and packaging, so investigating their mechanical properties such as elastic properties have attracted many researchers attention (Fattahi and Safaei 2017; Safaei and Fattahi 2017). Thakur et al.(2012), Showed by an experimental study that the stiffness, Young's modulus, wear resistance, toughness, and rigidity of high-density polyethylene (HDPE) matrix improves by the increasing volume fraction of carbon nanotube (CNT) as reinforcing fibre. Joshi and Upadhyay (2014) applied the numerical approach to analyse mechanical properties of polymeric nanocomposites reinforced with Multi-walled carbon nanotubes (MWCNTs) using methods based on continuous mechanics and volume element.

Furthermore, other investigations were conducted using various types of polymers as the matrix with different reinforcing fibres for specific purposes or application, for

✉ A. M. Fattahi
afattahi@uj.ac.za

1 Department of Mechanical Engineering Science, Faculty of Engineering and Built Environment, University of Johannesburg, Johannesburg, South Africa

example, Galgali et al. (2004) used polypropylene reinforced with nanoclay to examine the effect of nanoclay orientation on the tensile modulus of the produced nanocomposites as well as the relationship between nanoclay alignment and shear rate. Qian et al. (2000) showed by experimental that by adding only 1 wt% of the nanotube to the polyester resin, increases the elastic modulus of the nanocomposite by 35–42% and polymer strength by 25%. Zhu et al. investigated the tension-strain response of CNTs into the epoxy resins and proposed that by adding only 1–4 wt% of CNTs, increases the effective properties by 30–70%. Sharma and Nayak (2009) Investigated mechanical properties such as elongation at break, tensile modulus, tensile strength and the effect of organically modified clay on the morphological, thermal and physical properties of the nanocomposite. Wu et al. (2002) Studied the consequence of nanoparticle on different mechanical properties of polymer composite with low nanoparticle loadings at room temperature. The results showed the simultaneous improvement in the strength, elongation, and Young's modulus. Recently, several research works are conducted using CNTs as the reinforcing fibres for the determination of the electrical and mechanical properties of the resulting CNTs-based nanocomposite (Azizi et al. 2015a, b).

Griebel and Hamaekers (2004). Used molecular dynamics simulation to obtain the elastic modulus of polymer/CNTs nanocomposite and compered the elastic modulus results of their work with the rule of mixture results for long CNTs, pure polyethylene (PE) and CNTs surrounded by PE. Safaei et al. (2015). investigated the consequence of aspect ratio on the stress–strain reply of cohesively and the perfectly bonded HDPE/GNP nanocomposites. Barai and Weng (2011) investigated the effect of intermediate phase by first studying the properties of CNTs using the elastic equation where they considered a complete bond between polymer matrix and CNTs fibre and then observed high tension transfer from the matrix to the fibre. They then introduced the coefficient into their equation and calculated the effect of increasing the mentioned coefficient in the intermediate phase which resulted in the decrease in the effective Young's modulus of the composite. Najipour and Fattahi (2017) used the experimental approach to investigate the effect of adding CNTs nanoparticle on the mechanical properties of LDPE/CNTs nanocomposite and found that the hardness and the energy impact of the nanocomposite were improved. In the mentioned studies, only classic boundary conditions are considered. Accounting for non-classic boundary conditions commonly encountered in engineering applications, vibration analysis was also conducted on plates and shells reinforced by carbon nanoparticles under arbitrary boundary conditions (Qin et al. 2019a, b, 2020a, b), where the effects of nanoparticles together with boundary conditions

are evaluated. It is also shown through the existing literature that other researches such as Jalali et al. (2019) investigated the free vibration of the functionally graded (FG) microbeams using modified couple stress theory under thermal environment. Their results showed that an increase in FG index result with an increase in natural frequencies for low FG indexes, as for high FG indexes, the natural frequencies remained unchanged. Furthermore, it was observed that increasing the temperature change in the microbeam results with the decrease in the natural frequencies. Additional observation illustrated that the natural frequencies of the classical beam differ significantly from that of modified couple stress theory. Jalali et al. (2018) also investigated the effect of converging and diverging thickness profile of free rotating annular disc made of FG material on the natural frequencies and critical speed for specific boundary conditions. It showed that the high critical speed and natural frequency are obtained using a plate with a converging thickness profile, and the lower critical speed is obtained using a divergent thickness profile. It was also found that an increase in the ration of inner-outer radii is directly proportional to the critical aped of the FG annular disk. Mohammadsalehi et al. (2017) studied the effects of aspect ratio, boundary conditions structural damping coefficient, variable thickness parameters and nonlocal on the vibration features of variable rectangular nanoplates using nonlocal first-order shear deformation theory. It showed that increasing non-uniform parameter from 0 to 1, the natural frequencies increases. It was also found that the nanoplate structural damping coefficient is inversely proportional to the damping ratio. In addition, the increase in the plate edges constraint increases the nonlocal effect.

Based on our information, very little investigation work has been showed on the examination of the effect of different processing techniques and addition of SWCNTs to polymeric HDPE matrix on the elastic properties of HDPE/SWCNTs nanocomposites. The examination of elastic modulus, yield stress, the maximum force on the polymeric nanocomposites reinforced with SWCNTs nanoparticles and processed using two or more processing methods have attracted less attention of researchers. Therefore, in this work, injection and compression moulding method were used to process HDPE/SWCNTs nanocomposites at various weight fractions of SWCNTs.

Injection moulding is a popular technique that is extensively used in the manufacturing process to produce plastic components (Jahan and El-Mounayri 2016; Park et al. 2019). Compression moulding which is known as one of the oldest material processing methods for plastics is regarded as one of the first industrial techniques of moulding (Corbridge et al. 2017). Accordant to Kwon et al. (2018), Compression moulding method is known by

producing large and thin polymeric parts in a robust way. The effect of these two processing methods and the addition of SWCNTs nanoparticles into the HDPE matrix on the elastic properties of HDPE/SWCNTs nanocomposites samples were investigated. During the investigation, each test for the elastic properties of HDPE/SWCTs nanocomposite was repeated at least three times to obtain accurate average values for each factor. Finally, the elastic properties of HDPE/SWCNT nanocomposites were numerical analyzed using FEM approach for the approximation of the elastic modulus of nanocomposites. The results for both experimental and numerical were then compared and the concussions were made.

2 Experimental approach

2.1 Materials

In this study, HDPE was used as the matrix phase during the development of HDPE/CNT nanocomposite samples, and SWCNTs were used as the reinforcing fibres at various weight fraction. The HDPE/CNT nanocomposite samples were produce using two different processing methods as mentioned. The properties of the materials used are as follows:

The HDPE material was produced by Goodfellow Cambridge Limited at Huntingdon PE29 6WR England and provided by Sigma-Aldrich form 1 Friesland Drive, Longmeadow Business Estate South Modderfontein, Johannesburg 1645 South Africa. The properties of the HDPE used are presented in Table 1.

The SWCNTs material was produced by Sigma-Aldrich at 3050 Spruce Street. St. Louis. MO 63103 USA and has provided by Sigma-Aldrich 1 Friesland Drive, Longmeadow Business Estate South Modderfontein, Johannesburg 1645 South Africa. The properties of the used SWCNTs nanoparticles are presented in Table 2.

Table 1 The physical and chemical properties of HDPE used

Physical state	Clear to white pellets
Density	0.940 g/cm^3 or 940 kg/m^3
Weight impact	250 gm
Melting point temperature	125–135 °C
Flesh ignition temperature	335 °C
Auto ignition temperature	350 °C
Elongation at break	1000%
Yield strength	25 MPa
Odour	Slight waxy odour

Table 2 The physical and the chemical properties of SWCNTs used

Physical stat	Black fine powder
Density	1.68 g/cm^3 at 25 °C (lit.)
Bulk density	0.1 g/cm^3
Melting point temperature	3652–3697 °C (lit.)
Average diameter	10 nm
Median length	0.15 μm
Surface area	700 m^2/g
Impurities	5% Moisture content
Chirality	7.6
Purity/assay	90% carbon basis and 99% as carbon nanotubes
Elastic modulus	200 GPa

Table 3 The physical and the chemical properties of Maleic anhydride used

Physical stat	Clear to white pellets
Density	1.48 g/cm^3
Molar mass	98.06 g/mol
Melting point temperature	52.6 °C
Chem spider ID	7635
Boiling point	202 °C

Maleic anhydride Android was used as a compatibilizer to establish a great bond between the matrix and the fibres during the mixing process and its weight fraction was considered to be 1.25 in this study (De Roover et al. 1995). Table 3 provides the physical and chemical properties of the maleic anhydride used.

2.2 The preparation procedure

The weighting method was used to prepare pure and a mixture of HDPE/SWCNTs nanocomposite solutions at different SWCNTs nanoparticles weight fractions.

2.2.1 Preparation of pure HDPE samples

During the preparation of pure HDPE samples, 400 g of unprocessed HDPE pellets was measured using Stamp weighing scale. Pure HDPE was declared as 100% HDPE with 0 wt% of SWCNTs.

2.2.2 Preparation of HDPE/SWCNTs nanocomposites at different wt%

Preparation of HDPE/SWCNTs nanocomposites differ from that of pure HDPE since there is a mixing of HDPE

pellets and SWCNTs at various weight fractions. For this preparation SWCNTs, nanoparticles were added to the HDPE pellets together with maleic anhydride. Maleic anhydride was added into the mixture so that it can help to create a clear bond between HDPE and SWCNTs nanoparticles in HDPE/SWCNTs nanocomposites (Thakur et al. 2012; Hasegawa et al. 1998; De Roover et al. 1995). The following steps were followed during the preparation of HDPE/SWCNTs nanocomposites at 0.2 wt%, 0.4 wt%, 0.6 wt%, 0.8 wt% and 1 wt% SWCNTs nanoparticles weight fraction:

- Step 1: 5 g of maleic anhydride was measured using CAS weighing scale,
- Step 2: To attain HDPE/SWCNTs nanocomposites at the weight fraction of 0.2 wt%, 400 g of pure HDPE was multiplied with the given weight fraction of SWCNTs to calculate the mass of SWCNTs inside the nanocomposite. For example (400 g × 0.2% = 0.8 g) which gives 0.8 g of SWCNTs at the weight fraction of 0.2 wt%,
- Step 3: To calculate the mass of HDPE inside the HDPE/WSCNTs nanocomposites, masses of maleic anhydride and SWCNTs were subtracted from 400 g were mass of maleic anhydride was kept at 5 g. For example (400–5–0.8 g = 394.2 g) which gives 394.2 g of HDPE at the weight fraction of 0.2 wt%,
- Step 4: HDPE reinforced with SWCNTs nanoparticles at the weight fraction of 0.2 wt% was then performed by measuring 394.2 g of HDPE, 5 g of maleic anhydride and 0.8 g of SWCNTs nanoparticles and then added into one beaker and mixed with the steering rod.

Figure 1 summarises the steps of the mixing procedure conducted to produce the pure HDPE and HDPE/SWCNTs nanocomposites and the measurement for each weight fraction of SWCNTs are presented in Table 4.

The preparation of HDPE/SWCNTs and the weight fraction of 0.4 wt%, 0.6 wt%, 0.8 wt%, and 1 wt% was conducted according to the given steps. Table 4
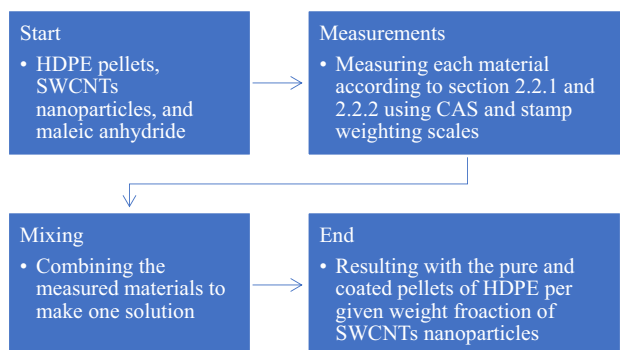

Fig. 1 Flow diagram of the mixing procedure

summarizes the preparation parameters for all the weight fractions of SWCNTs nanoparticles. Since the experimental analysis was focusing on the two processing techniques, the experimental was design according to the Taguchi's method. In this study, the Taguchi method has been used to assess the results of the tensile test and draw the conclusions of the experimental results. Taguchi's technique is among the most general approaches of statistical analysis (Najipour and Fattahi 2017). The SWCNTs weight fractions in six levels and the processing techniques in two levels were considered. According to Taguchi's method, twelve experiments were designed. The parameters and levels are shown in Table 4.

2.3 Specimens

In order to examine the effect of injection moulding, compression moulding and the addition of SWCNTs wt% on the elastic properties of HDPE/SWCNTs nanocomposites, the tensile test specimen was produced through injection and compression moulding. The tensile test samples were produced through the injection and compression moulding according to the ASTM standard D638-14. The preparation of tensile test samples for both processing methods at the given weight fractions of SWCNTs was conducted using the flow diagram in Fig. 2.

According to the flow diagram in Fig. 2, the processing of the HDPE/SWCNTs nanocomposite tensile test samples started with the coated pellets that were prepared regarding Table 4. The pellets were fed into the twin-screw extruder for melting and mixing which was operating at the temperature ranging from 170 to 190 °C, the screw rotating speed of 250 RPM and the pressure of 120 MPa. This was done independently for the HDPE/SWCNTs pellets of the same weight fraction. From the extruding process, each group of mixed HDPE/SWCNTs composites came out as the homogeneous stripes of nanocomposite that were cooled through the water at the temperature of 25 °C and then cut into small pellets ageing using a grinder. The milled pellets were then dehumidified at the temperature of 60 °C for 9 h using the oven. This was done to prepare all the of pure HDPE and the HDPE/SWCNTs composites pellets for the injection and compression moulding.

Each group of pure HDPE and HDPE/SWCNTs composites at the given weight fractions was prepared for the injection and compression mounding. For the injection moulding, the pellets were nursed into the plastic injection machine that was operated at the injection pressure of 9 MPa, regulation temperatures of 175 °C, 190 °C, and 200 °C. For compression moulding, the pellets were processed at the compression pressure of 2000 N, with the upper heater plate at 197 °C and the lower heated plate at 194 °C. The tensile test samples from both processing

Table 4 The experimental designed according to the Taguchi's approach

Sample number	SWCNTs weight fraction (wt%)	Processing methods	HDPE mass (g)	Maleic anhydride mass (g)	SWCNTs mass (g)
1	0	Injection moulding	400.0	0	0
2	0	Compression moulding	400.0	0	0
3	0.2	Injection moulding	394.2	5	0.8
4	0.2	Compression moulding	394.2	5	0.8
5	0.4	Injection moulding	393.4	5	1.6
6	0.4	Compression moulding	393.4	5	1.6
7	0.6	Injection moulding	392.6	5	2.4
8	0.6	Compression moulding	392.6	5	2.4
9	0.8	Injection moulding	391.8	5	3.2
10	0.8	Compression moulding	391.8	5	3.2
11	1	Injection moulding	391.0	5	4
12	1	Compression moulding	391.0	5	4

Fig. 2 The processing flow diagram
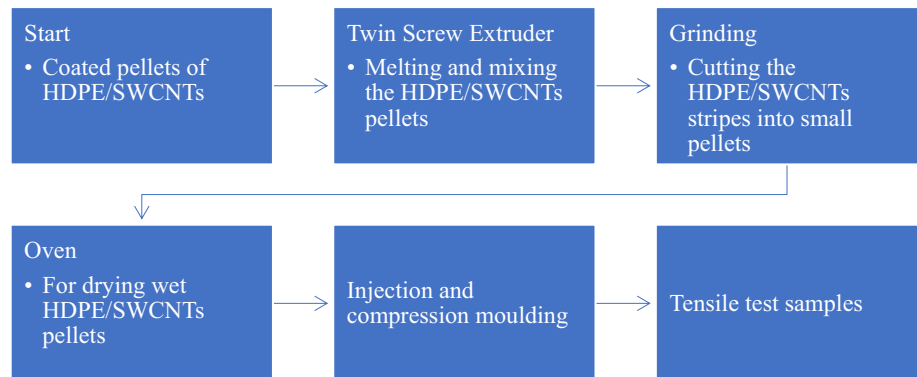
methods were produced according to the ASTM and ISO 527-1 standard for measurement type 1. With the dimensions given as: the length overall (LO) of 165 mm, width overall(WO) of 19 mm, length of narrow section (L) of 57 mm, width of narrow section (W) of 13 mm, thickness (T) of 3.2 ± 0.4 mm, and Radius of fillet (R) of 76 mm. This was constant for all processed samples in both processing techniques. The resulting samples are presented in Fig. 3.

For each processing method and weight fraction, five tensile test samples of HDPE/SWCNTs were made. The was performed so that other samples can be used for the validation for experimentation as well as the calibration of the machine before the main experiment.

2.4 Experimental analyse

2.4.1 Experimental setup

The tensile tests were conducted according to the ASTM D638-14 and ISO 527-1 for plastics. The tensile test machine used is Zwick/Roell Z250 in Fig. 4. It was set to the following regulating parameters; grip to grip distance at the initial position of 83 mm, starting position speed of 5 mm/min, pre-load of 0.1 MPa and the pre-lead speed of mm/min. The testing parameters were kept constant for all tested samples.
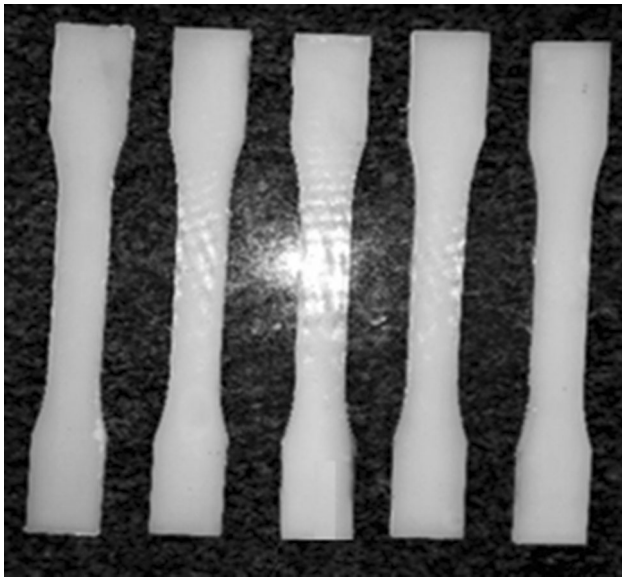
Fig. 3 Tensile test samples of HDPE/SWCTs nanocomposites (wt% = 0)

2.4.2 Experimental results

During the experiment, three tensile tests for each weight fraction and processing method were conducted according to the experimental matrix in Table 4. The average elastic modulus of the three tensile tests and their standard deviation are presented in Table 5.

The tensile test results in Table 5. Are summarized in Fig. 5. To help demonstrate the relationship between the two processing techniques and the addition of the SWCNTs

into HDPE matrix. However, Table 5. Presents the average elastic modulus of pure HDPE for both injection and compression moulding as 581.198 MPa and 534.855 MPa respectively. According to the MatWeb (2013) and Huang et al. (2013) the average elastic modulus of pure HDPE, ranges form 0.450 to 1.50 GPa depending on the way it is processed including the variations of temperature, pressure and other factors that might affect these properties. This shows that the results in Table 5 are within the range and they are acceptable.

The results in Fig. 5. Shows that the average elastic modulus of HDPE/SWCNTs nanocomposite is directly proportional to the addition of SWCNTs nanoparticles into the HDPE matrix per processing method. Furthermore, it shows that injection moulding yield high average elastic modulus compared to compression moulding per given weight fraction of SWCNTs nanoparticles. Statistically, Injection moulding compared to compression moulding at the 0 wt% of SWCNTs yield 9% ("Appendix 1") improvement in average elastic modulus of pure HDPE, and at the 1 wt% injection moulding yield 14% ("Appendix 1") improvement in average elastic modulus of HDPE/SWCNTs nanocomposite computer to that of compression moulding.

The results in Fig. 5, compare the effect of processing methods on the elastic modulus of HDPE/SWCNTs nanocomposite. However, they do not consider the effect of the addition of SWCNTs nanoparticles on the elastic modulus of HDPE/SWCNTs nanocomposites. To examine the effect of the addition of SWCNTs nanoparticles on the average elastic modulus of HDPE/SWCNTs

Fig. 4 The Zwick/Roell Z250 tensile testing machine

Table 5 Tensile test results

Sample number	SWCNTs weight fractions (wt%)	Elastic modulus (MPa)			Average elastic modulus (MPa)	Standard deviation
		Teat 1	Test 2	Test 3		
1	0	545.881	579.671	618.044	581.198	29.480
2	0	550.545	500.441	553.579	534.855	24.366
3	0.2	594.272	562.010	604.866	587.050	18.226
4	0.2	564.607	571.933	472.906	536.482	45.055
5	0.4	573.793	643.710	588.833	602.114	30.051
6	0.4	502.837	667.260	519.568	563.222	73.882
7	0.6	588.843	589.317	666.981	615.047	36.723
8	0.6	595.185	582.773	535.370	571.109	25.775
9	0.8	577.004	667.450	690.309	644.921	48.923
10	0.8	615.141	607.285	526.915	583.114	39.868
11	1	748.498	720.125	742.473	737.032	12.206
12	1	815.630	604.502	525.045	648.392	122.623
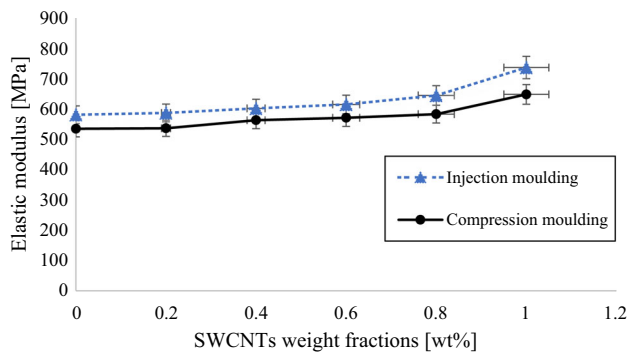
Fig. 5 Effect of SWCNTs on the elastic modulus of HDPE/SWCNTs processed with two different techniques

nanocomposite, Taguchi's signal to noise ratio *S/N* method was implemented. *S/N* is a loss function the is normally introduced to compete for the effect of two or more parameters on a given output (which in elastic modulus in this case). Equation 1 represents the signal to noise ratio *S/N*:

$$\frac{S}{N} = -10 \log\left(\frac{1}{n}\sum_{i=1}^{n}\frac{1}{y_i^2}\right) \quad (1)$$

where, *n* is the number of the observation on the specific product and *y* is the respective characters representing the average elastic modulus *E* of HDPE/SWCNTs nanocomposite. S/N method was used in Table 6, to examine the outcome of the addition of SWCNTs nanoparticle weight fraction into HDPE matrix and the processing techniques on the average elastic modulus of HDPE/SWCNTs nanoparticles.
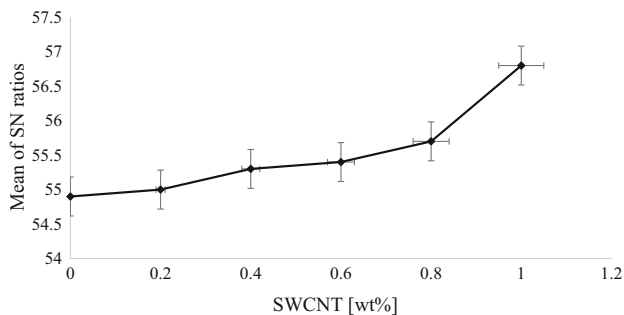
The investigated parameters in Table 6, are the effects of SWCNTs weight fraction and the processing methods on the average elastic modulus of HDPE/SWCNTs nanocomposites using signal to noise ratio. The average elastic modulus nanocomposite in six levels and the processing methods in two levels were considered since there were six variations of SWCNTs weight fractions and two processing methods used. The signal to noise ratio results was obtained according to Table 6, where Δ is the difference between the largest and the smallest data. Rendering the Taguchi's method, the parameter with the biggest S/N has a major effect on the experiment. Figure 6, characterizes the mean S/N at given SWCNTs weight fractions.

According to the signal to noise results analysis obtained in Table 6, the addition of weight fraction of SWCNTs had a more significant effect on the average elastic modulus of HDPE/SWCNTs nanocomposite sample compared to the processing methods applied. The addition of SWCNTs up to 1 wt% resulted in an important increase in the average elastic modulus of 24% ("Appendix 1"), with the highest average values of elastic modulus and signal to noise ratio at level 6. Figure 6, present the relationship between the SWCNTs nanoparticle weight friction and the mean S/N ratios. Is display that addition of SWCNTs weight fraction of result with the vital increase in the mean S/N ration which shows an increase in the average elastic modulus of HDPE/SWCNTs nanocomposite. This is due the evident that adding SWCNTs nanoparticles into the HDPE matrix has more effect on the modulus of elasticity of HDPE/SWCNTs nanocomposites.

Figure 7, which was generated from Table 6, demonstrates the effect of an injection and compression moulding on the average elastic modulus of HDPE/SWCNTs
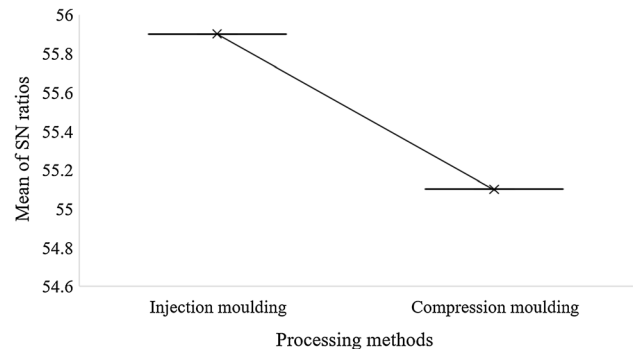
Table 6 Signal to noise ratio S/N for tensile strength data

Effect of SWCNTs weight fraction (wt%)			Effect of processing methods		
Level	Elastic modulus (MPa)	$\frac{S}{N} = -10\log\left(\frac{1}{2}\sum_{i=1}^{2}\frac{1}{E_i^2}\right)$	Level	Elastic modulus (MPA)	$\frac{S}{N} = -10\log\left(\frac{1}{6}\sum_{i=1}^{6}\frac{1}{E_i^2}\right)$
1	$E_1 = 581.198$ $E_2 = 534.855$	54.9	1	$E_1 = 581.198$ $E_2 = 587.050$ $E_3 = 602.114$ $E_4 = 615.047$ $E_5 = 644.921$ $E_6 = 737.032$	55.9
2	$E_1 = 587.050$ $E_2 = 536.482$	55.0			
3	$E_1 = 602.114$ $E_2 = 563.222$	55.3			
4	$E_1 = 615.047$ $E_2 = 571.109$	55.4	2	$E_1 = 534.855$ $E_2 = 536.482$ $E_3 = 563.222$ $E_4 = 571.109$ $E_5 = 583.114$ $E_6 = 648.392$	55.1
5	$E_1 = 644.921$ $E_2 = 583.114$	55.7			
6	$E_1 = 737.032$ $E_2 = 648.392$	56.8			
Δ	$56.8 - 54.9 = 1.9$		$55.9 - 55.1 = 0.8$		
Rank	1		2		

Fig. 6 Average S/N against the addition of SWCNTs nanoparticles into HDPE matrix

Fig. 7 Mean of S/N ratios of the two processing methods

nanocomposites. It shows that injection moulding indeed has more effect compared to compression moulding as illustrated in Fig. 5.

During the experiment, other tensile properties such as the yielding stress, yielding point elongation and maximum force for both injection and compression moulding methods were investigated and their results are presented in Tables 7 and 8 respectively.

The data in Tables 7 and 8 were used to generate Figs. 8, 9 and 10 in order to assist to compare the yield stress, elongation, and the maximum force for the HDPE/SWCNTs samples produced through injection and compression moulding as the weight fraction of SWCNTs increases.

Figures 8 and 9, shows the similar characteristics which demonstrate both the yield stress and the maximum force
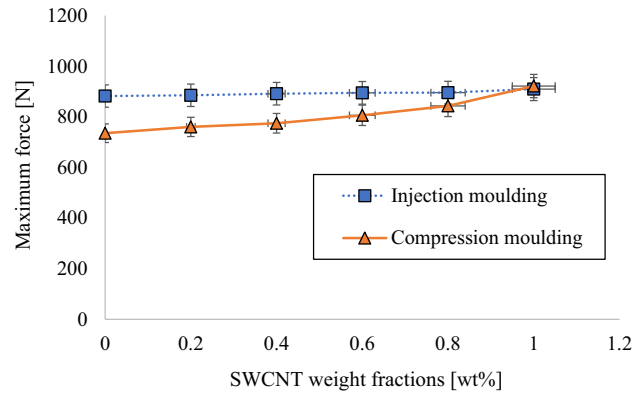
Table 7 Tensile properties for injection moulding HDPE/SWCNTs nanocomposite samples

SWCNTs weight fractions (wt%)	Yielding stress (MPa)	Elongation at yield point (%)	Maximum force (N)
0	23.156	9.038	882.242
0.2	23.237	15.088	885.330
0.4	23.399	11.907	891.499
0.6	23.490	11.071	894.963
0.8	23.510	10.875	895.727
1	23.879	11.362	909.796

Table 8 Tensile properties for compression moulding HDPE/SWCNTs nanocomposite samples

SWCNTs weight fractions (wt%)	Yielding stress (MPa)	Elongation at yield point (%)	Maximum force (N)
0	19.305	5.763	735.505
0.2	19.954	5.804	760.260
0.4	20.336	6.711	774.785
0.6	21.162	6.912	806.264
0.8	22.138	6.293	843.464
1	24.194	7.410	921.788
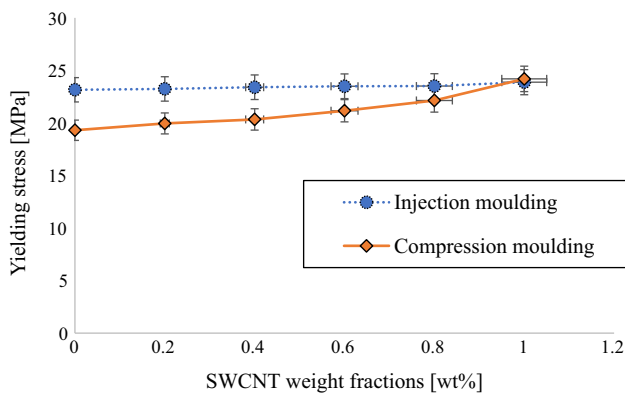
Fig. 8 Variation of the yield stress of HDPE/SWCNTs nanocomposites for both processing methods with SWCNTs weight fraction

Fig. 9 Variation of the maximum force of HDPE/SWCNTs nanocomposites for both processing methods with SWCNTs weight fraction
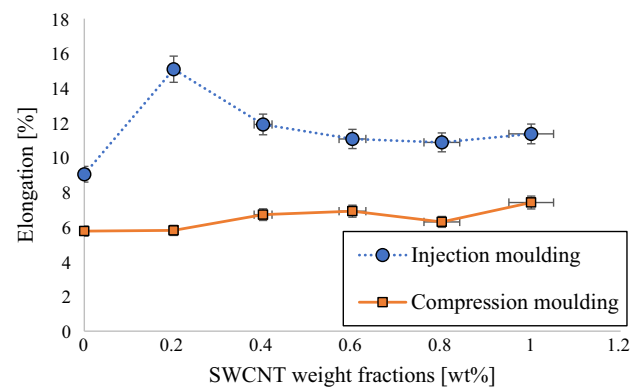
Fig. 10 Variation of the ultimate elongation of HDPE/SWCNTs nanocomposites for both processing methods with SWCNTs weight fraction

of HDPE/SWCNTs nanocomposites produced using two various method and different weight fractions of SWCNTs. Together they show that the injection moulded samples of HDPE/SWCNTs nanocomposite display hardly any change in yield stress and maximum force at different wt% fractions. Furthermore, compared to compression moulded samples, the injection moulded samples contain higher yield stress and the maximum force from 0 wt% until 0.8 wt% of SWCNTs. At 1 wt%, the compression moulded samples show an improvement in yield stress and maximum force. In overall, the yield stress and the maximum

force of HDPE/SWCNTs nanocomposite samples increases for both processing methods as the weight fraction of SWCNTs increased in the HDPE matrix. However, compression moulded samples show better improvement at high SWCNTs weight fractions.

Figure 10, display the variation of the ultimate elongation percentage of HDPE/SWCNTs nanocomposite samples at various SWCNTs weight fractions for injection and compression moulding. Compared to compression moulded HDPE/SWCNTs nanocomposite samples, Injection moulded samples shows high but fluctuating results of ultimate elongation percentage. These show that the elongation of the HDPE/SWCNTs nanocomposite does not depend on the weight fraction of SWCNTs. However, the average injection moulded HDPE/SWCNTs nanocomposite samples elongate more compare to the compression moulded samples.

In general, the tensile test experimental results for both processing methods at the same increment of SWCNTs weight fractions showed that compare to compression

moulding, injection moulding has more effect on the improvement of elastic modulus of HDPE/SWCNTs nanocomposites. Furthermore, the tensile results showed that the adding of SWCNTs nanoparticles into pure HDPE at concentrations up to 1 wt%, has major effect than the two processing techniques on the improvement of the elastic properties of HDPE/SWCNTs nanocomposites. Having stated the experimental observation, it is always imported to perform further examinations to verify the results obtained since the experimental result are not always accurate due to the following: The challenges in finding the better approach of mixing HDPE matrix and SWCNTs nanoparticles for good distribution of the nanoparticle through the matrix, errors encountered during the processing methods, experimental errors due to the equipment operations or human errors during the experimentation and other factors the can affect the outcome. Excluding the errors that could be encountered during experimentation, experimental approach its self is costly and time-consuming. An approach such as numerical FEM which is fast and less expensive was used for the validation and to minimize the errors in the experimental result.

3 Numerical approach

Numerical approaches incorporated computer software to help to solve complex mathematical problems that are hard to solve analytically (Hoffman 2018). The numerical solutions are regarded as approximate, and they can be accurate in some cases. This section of the study presents the finite element method (FEM) solution for the validation of the elastic modulus of HDPE/SWCNTs nanocomposite at the different weight fractions of SWCNTs nanoparticles. The representative volume element (RVE) method was introduced to achieve this. The RVE plays an important role in the physics and the mechanics of random heterogeneous materials when it includes understanding and computing their effective properties (Kanit et al. 2003). Since HDPE/SWCNTs nanocomposites are heterogeneous materials with the SWCNTs nanoparticles randomly

scattered nanoparticles through the HDPE matrix, then the RVE is the useful method this investigation.

3.1 Finite element method (FEM)

FEM is an arithmetical technique used to solve mathematical, engineering and physics problems such as fluid flow, heat transfer, structural analysis and others (Dehghani et al. 2003; Horritt and Bates 2001). In this study, structural analysis was useful to solve the elastic properties of the HDPE/SWCNTs nanocomposites at a various weight fraction of SWCNTs. The elements types used in this study for the modelling of the HDPE matrix, intermediate phase, and SWCNTs fibre are the same one applied by Fattahi et al. (2018). The FEM approach implemented by Tebeta et al. (2019) was applied to help for the modelling and predicting of the elastic modulus of HDPE/SWCNTs nanocomposites. Figure 11 present the element types used in FEM.

Figure 11, illustrate the 3D tension elements of C3D83R which was used to represent the solids elements (HDPE matrix and SWCNTs fibre) and for the intermediate phase, which is the bond between solid elements, the adhesive element of COH3D8 was implemented. In most studies the intermediate phase is treated as the spring bonds between the matrix and the fibre for more accurate numerical FEM simulations and for some investigation is ignored (Fattahi et al. 2018). However, in this study, the intermediate phase was presented as the thin bond existing between fibre and matrix to improve the model and to understand the interaction of matrix and fibre in the nanocomposite. The properties of the type of the intermediate phase used were obtained from the atomic simulation results of Namilae and Chandra (2005). Where the separate region was created between the matric and fibre in the form of a tube to assign the area and the properties of the intermediate phase. This physical separation between the matrix and fibre does not mean the existence of third material or a phase. However, the adjustment for modelling force transfer properties from the matrix to the fibre.

The atomic simulation results of Namilae and Chandra (2005), were conducted as follows: A displacement of 0.05

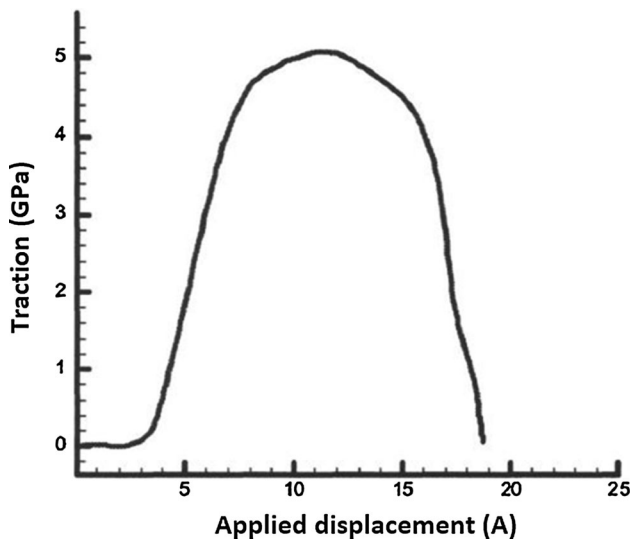**Fig. 11** The elements types used for modelling (Safaei et al. 2018)
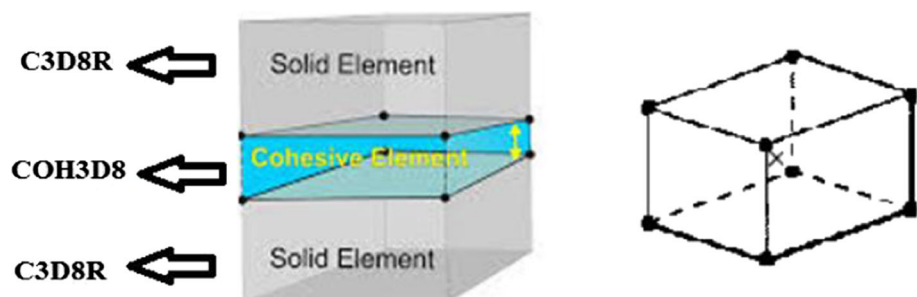
Fig. 12 Atomic simulation traction movement plot (Fattahi et al. 2018)

Å was assigned to the terminal atoms of the CNTs with the main length of 15 Å. The system was set to balance for a 150-time interval of 0.2 Fs for each displacement. These simulations were performed until some hydrocarbon chains of CNTs terminals split, and these processes generally take 500,000–800,000-time intervals. Figure 12 present the results of the simulation where the slope of the primary section yields the hardness to length units of the intermediate phase which was used to determine the intermediate phase elastic modulus according to the Eqs. 2, 3, and 4.

$$M = \frac{(0.1 - 0)}{(3 - 0)} = 0.03333 \frac{\text{GPa}}{\text{Å}} \tag{2}$$

$$L_{CNT} = 122\,\text{Å} \tag{3}$$

where M and L_{CNT} are the gradient of the graph and length of CNT element which was assumed to be 122 Å because of molecular dynamics results. The elastic modulus of the intermediate phase was then calculated as E_i by multiplying the primary slope of the graph which is from zero to 5 Å with the length of CNT to yield the following:

$$E_i = M \times L_{CNT} = 0.03333 \frac{\text{GPa}}{\text{Å}} \times 122\,\text{Å} = 4.06\,\text{GPa} \tag{4}$$

The region of the primary slope which is from zero to 5 Å was selected because it seemed to be reasonable for the maximum displacement of 0.5. Other results obtained are thickness and Poisson's ratio of the intermediate phase as 0.4 nm and 0.3 respectively. These properties were applied for the modelling of the HDPE matrix reinforced with SWCNTs using RVE.

3.2 Represented volume element (RVE)

The RVE that present the investigated section HDPE/SWCNTs nanocomposites was generated according to the test section of the tensile test geometry presented in Fig. 13. Where the green region on the test segment of the tensile test specimen is assumed to be microscopic cut through showing randomly scattered red nanoparticle.

Figure 13, shows the SWCNTs nanoparticles presented in red at the test segment of the geometry which they are presumed to be homogeneously dispersed and surrounded by HDPE matrix. It also assumed that there is no occurrence of SWCNTs nanoparticles combination through the nanocomposite (Tebeta et al. 2019). The magnified section in Fig. 13, represent the RVE which shows to consist of three phases that are HDPE matrix, intermediate phase, and SWCNT fibre. According to the existing researches and literature, SWCNTs nanoparticles are normally modelled as nanofibers enclosed by the intermediate phase regions which exist between the matrix and the fibre (Ahmadi et al. 2019; Ngabonziza et al. 2011; Wang et al. 2016; Thomas and Roy 2016; Hassanzadeh-Aghdam et al. 2018). Figure 14, present the two views and the boundary conditions of the enlarged HDPE/SWCNTs nanocomposite RVE.

It was assumed that the RVE in Fig. 14 experience the same load applicational as the tensile test geometry presented in Fig. 13, which are the fixed region on the right end and the applied load on the other. The effect of SWCNTs nanoparticle weight fraction on the REV is modelled in the next section.

## 3.3 HDPE/SWCNTs nanocomposites RVE modelling

HDPE/SWCNTs nanocomposite is made of two materials of different properties and the intermediate phase as mentioned. Table 9, contains the dimensions and properties of the SWCNTs nanoparticles, HDPE and the intermediate phase used for the nanocomposite. The HDPE matrix in Table 9, have to different elastic modulus which is obtained from the average experimental results for pure HDPE processed by Injection and completion moulding respectively. The elastic modulus of SWCNTs nanoparticles was obtained from Table 2.

Figure 15 characterize the dimensions of the RVE where SWCNTs length is 150 nm with the internal diameter of 9.2 nm and the external diameter of 10 nm. The x parameter represents the thickness of the HDPE matrix around the reinforcing fibre and it changes with the weight fraction. For every weight fraction of SWCNTs nanoparticle, the value of x parameter will give the dimensions of the RVE.

Fig. 13 Tensile test sample geometry
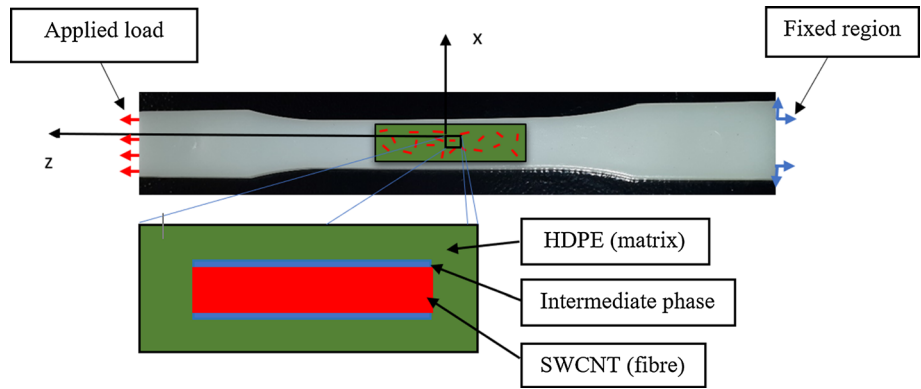
Fig. 14 Enlarged RVE boundary conditions
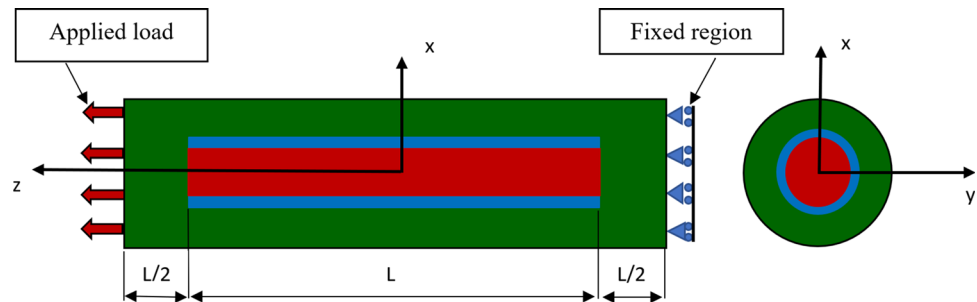
Table 9 Dimension and the properties of the HDPE/SWCNTs nanocomposite RVE (Fattahi et al. 2018)

Properties	Intermediate phase	(HDPE) matrix	(SWCNTs) fibre
Initial length (nm)	150		150
Initial internal radius (nm)	5	Change with x	4.6
Initial outer radius (nm)	5.4		5
Elastic modulus	4.06 (GPa)	581.198 and 534.855 (MPa)	200 (GPa)
Poisson's ration	0.3	0.3	0.3
Density (g/cm^3)	–	0.940	1.68

Fig. 15 Typical dimensions of RVE of HDPE/SWCNTs nanocomposite
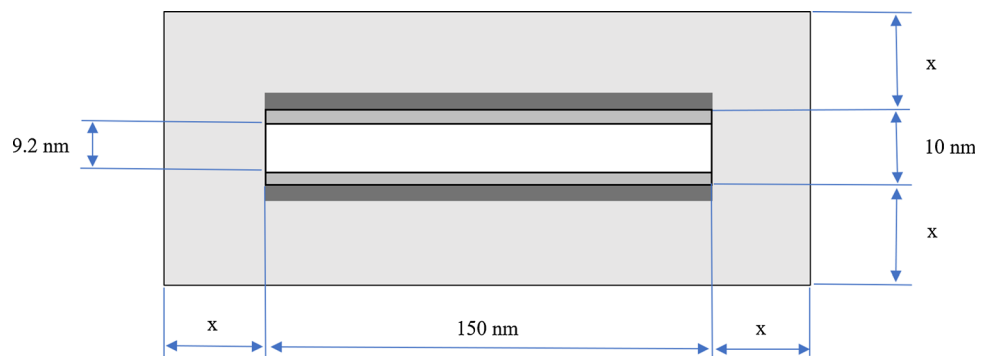
To calculate the x parameter in Fig. 15. The dimension and the properties in Table 11, were applied in the Eqs. 5, 6, and 7 at the SWCNTs weight fractions of 0.2 wt%, 0.4 wt%, 0.6 wt%, 0.8 wt% and 1 wt%. This was performed to calculate the value of x limit for each wt% specified as follows:

$$V_{SWCNT} = \pi\left((5)^2 - (4.6)^2\right)(150) = 576\pi \tag{5}$$

$$V_{RVE} = \pi\left(\left(\frac{2x + 10}{2}\right)^2\right)(2x + 150) \tag{6}$$

where V_{SWCNT} and V_{RVE} are the volume of SWCNT

Table 10 The dimension of RVE for different weight fraction of SWCNT (Tebeta et al. 2019)

SWCNTs weight fraction (wt%)	Volume fraction	Parameter x (nm)	The diameter of RVE (nm)	The length of RVE (nm)
0.2	0.112	41.90	93.80	233.80
0.4	0.224	29.99	69.98	209.98
0.6	0.337	24.33	58.66	198.98
0.8	0.449	20.87	51.74	191.74
1	0.562	18.42	46.84	186.84

Fig. 16 Boundary conditions of a quarter of HDPE/SWCNTs nanocomposite RVE
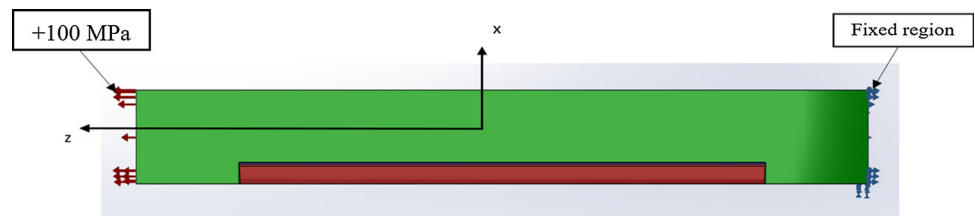
nanoparticle inside HDPE matrix the volume of RVE of the HDPE/SWCNTs nanocomposite respectively. These two equations are related by 3 as:

$$V_f = \frac{V_{SWCNT}}{V_{RVE}} = \frac{wt\%}{wt\% + \left(\frac{\rho_f}{\rho_m}\right)(1 - wt\%)} \qquad (7)$$

where V_f, $wt\%$, ρ_f and ρ_m are the volume fraction, the SWCNT fibre weight fraction, the density of SWCNT fibre, and the density of an HDPE matrix respectively.

The results of Eqs. 5, 6, and 7 give Eqs. 8. Which was simplified to give the third-order Eq. 9 as:

$$V_{RVE} = \frac{V_{SWCNT}}{V_f} \times 100 = \pi \left(\left(\frac{2x+10}{2} \right)^2 \right)(2x + 150)$$
$$= \frac{576\pi}{V_f} \times 100$$
$$(8)$$

$$2x^3 + 170x^2 + 1550x + 3750 = \frac{576}{V_f} \times 100 \qquad (9)$$

The value of x parameter for each specified weight fraction SWCNT was found by calculating Eq. 9. The obtained values of x parameters were then substituted in Eq. 10 to solve the diameters and the lengths of the RVE for each SWCNTs weight fraction.

$$D_{RVE} = 2x + 10, \quad L_{RVE} = 2x + 150, \qquad (10)$$

where D_{RVE} and L_{RVE} are the diameter and the length of RVE respectively. Table 10 summarises the result for the dimension of the RVE of HDPE/SWCNTs nanocomposite for a given SWCNT weight fraction.

3.4 Numerical simulation of the RVE

The RVE dimensions in Table 10 and the properties in Table 9 were used to generate the HDPE/SWCNTs nanocomposite model using ANSYS software. The input and assumptions made during the FEM model of the RVE on ANSYS 19.2 Mechanical APDL were as follows: The setting of preferences was adjusted to structural analysis, the element type selected was solid 10 nodes 187, the material was assumed to be rigid, elastic, linear, and isotropic. The model was shaped as a quarter of a cylinder as demonstrated in Fig. 16. Since is symmetrical. The applied load was set to be 100 MPa and the boundaries are as shown in Fig. 16.

The meshed geometry of RVE is presented in Fig. 17. With the load application and two longitudinal edges in z-direction assumed as symmetric. The mesh size of the model was improved by mesh validation form the size of 10–1 nm, and it is shown in Fig. 18 that the mesh size from 6 nm to 1 nm began to stable. According to Moaveni (Moaveni 2003) the smaller the mesh size the better the FEM simulation results (Fig. 17).

The mesh size of 2 nm was selected since is closer to the smallest mesh size and is within the range of stabilization. The mesh results in Fig. 18 were obtained using the parameters of injection moulded HDPE/SWCNTs nanocomposite samples at the SWCNTs weight fraction of 0.8 wt%. Figure 19 present fine mesh of 2 nm that was used for the simulation of HDPE/SWCNTs nanocomposite RVE for all weight fractions of SWCNT.

3.5 Numerical results

The modelling results obtained from the FEM model presented, for both injection and compression moulding are

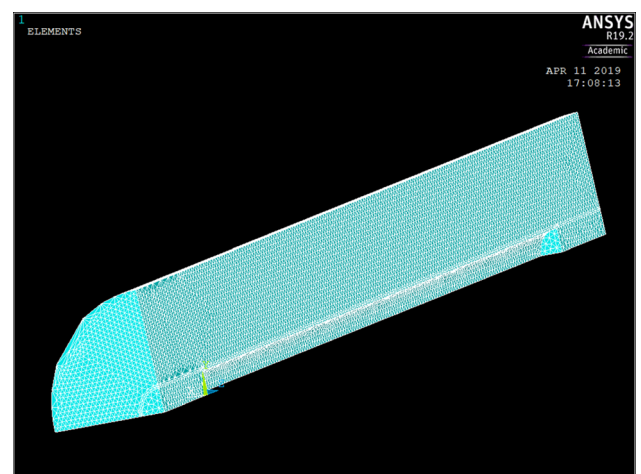**Fig. 17** Meshed geometry of the RVE
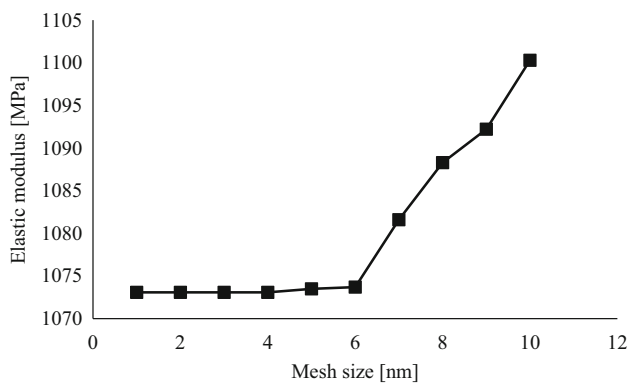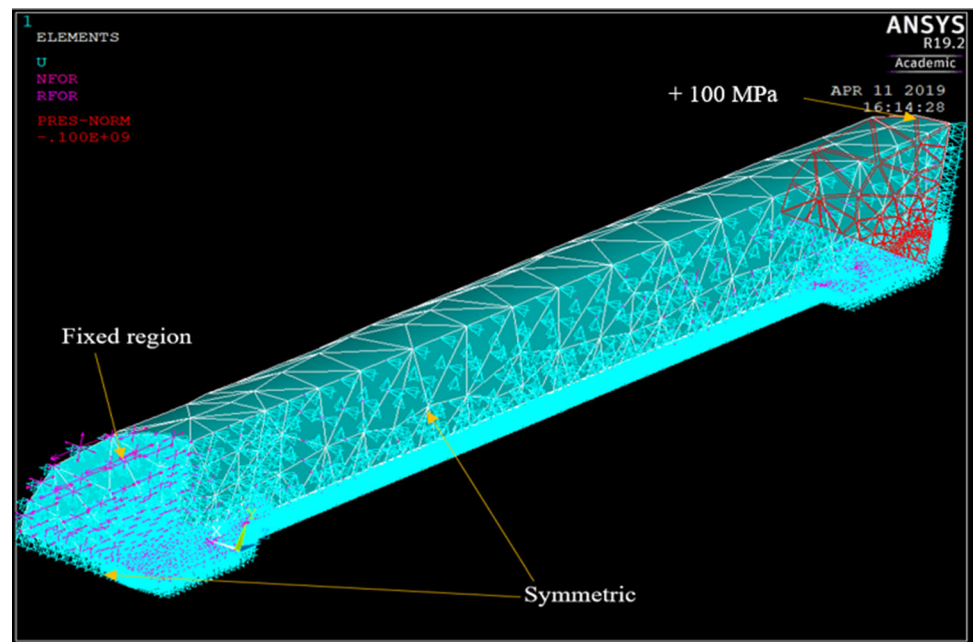
Fig. 18 Mesh independence of HDPE/SWCNT nanocomposite RVE

Fig. 19 Fine meshed geometry of the RVE

summarized in Table 11. These results were achieved using the model presented in Sect. 3.3. The elastic modulus of HDPE/SWCNTs nanocomposite for both processing techniques was calculated using the RVE nodal displacement and the nodal stress transfer of the model as presented in Figs. 20 and 21.

The elastic modulus of simulated HDPE/SWCNTs nanocomposite RVE for both processing methods were obtained using Eq. 11 as follow:

$$E_c = \frac{PL}{DMX} \tag{11}$$

where E_c is the nanocomposite elastic modulus, P is the load applied to the RVE (100 MPa), L is the HDPE/SWCNT nanocomposite RVE length per given SWCNTs weight fraction, and DMX is the FEM simulated maximum displacement of the RVE which also change with the
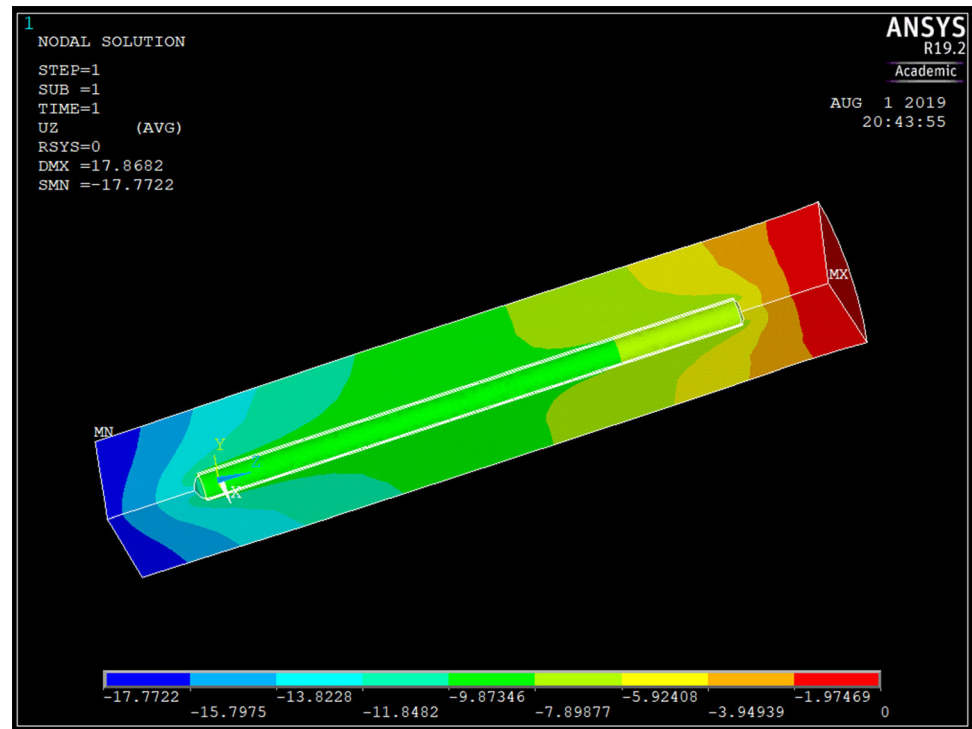
SWCNTs weight fraction. The FEM simulation results for the elastic modulus of HDPE/SWCNT nanocomposite RVE for both processing methods at specified weight fractions of SWCNTs are summarized in Table 11.

Figure 22 display the relationship between the numerical FEM simulated elastic modulus results of HDPE/SWCNTs nanocomposites for both processing methods at various weight fractions of SWCNTs nanoparticles. The FEM results showed that the HDPE/SWCNTs nanocomposites elastic modulus for both processing approaches increases as the SWCNTs weight fractions increases. Furthermore, the numerical FEM results showed that the HDPE/SWCNTs nanocomposite processed with injection moulding has higher elastic modulus for every given

Table 11 The FEM simulated HDPE.SWCNTs nanocomposites RVE elastic modulus results

SWCNTs weight fraction (wt%)	Injection moulding FEM (MPa)	Compression moulding FEM (MPa)
0.2	717.427	664.038
0.4	846.405	781.992
0.6	968.791	902.139
0.8	1073.080	1005.693
1	1247.596	1112.084

**Fig. 20** Maximum nodal displacement of the RVE in the z-direction


SWCNTs weight fraction compared to the compression moulding elastic modulus. These results correspond to the tensile experimental results presented in Fig. 5.

4 Comparison of the results

The experimental and numerical FEM elastic modulus results of HDPE/SWCNTs nanocomposites for both processing methods at the given weight formations of SWCNTs nanoparticles summarized in Tables 5 and 11 were compared respectively. Figures 23 and 24 were generated from Tables 5 and 11 to present the relationship between the experimental and numerical FEM for the elastic modulus of HDPE/SWCNTs nanocomposites processed by injection and compression moulding correspondingly.

Figures 23 and 24, shows that by increasing SWCNTs nanoparticles weight fractions into the HDPE matrix, the elastic modulus results for both experimental and numerical FEM increases for both processing techniques. Furthermore, among the important consultations was that increasing SWCNTs weight fraction, the errors between the experimental and numerical approaches were increased. This is because according to the numerical FEM results, as the SWCNTs nanoparticles weight fraction increases, the HDPE/SWCNTs nanocomposite elastic modulus was improved while in experimental results were improved but not as much as using a numerical approach. This is since during the experimentation, errors, as mentioned before, were encountered, and the other factor might be due to the agglomerating occurred during the addition of SWNNTs nanoparticles into HDPE matrix which in turn resulted in high errors in the experimental elastic modulus results.
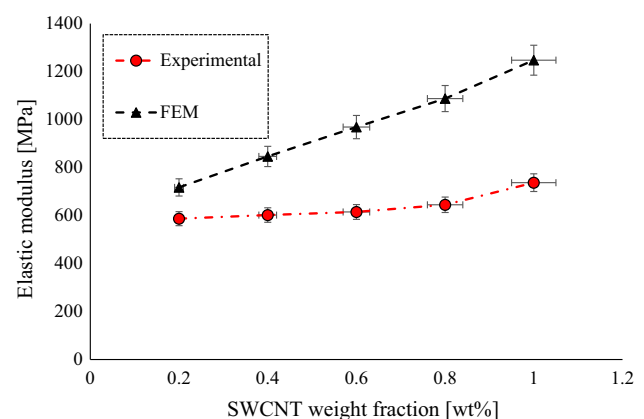
Fig. 21 Maximum stress transfer in the RVE of HDPE/SWCNT nanocomposite
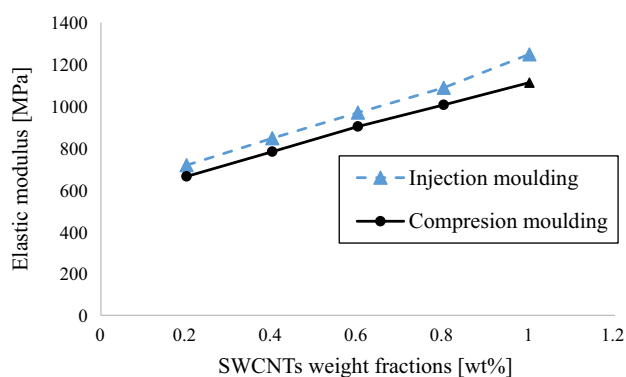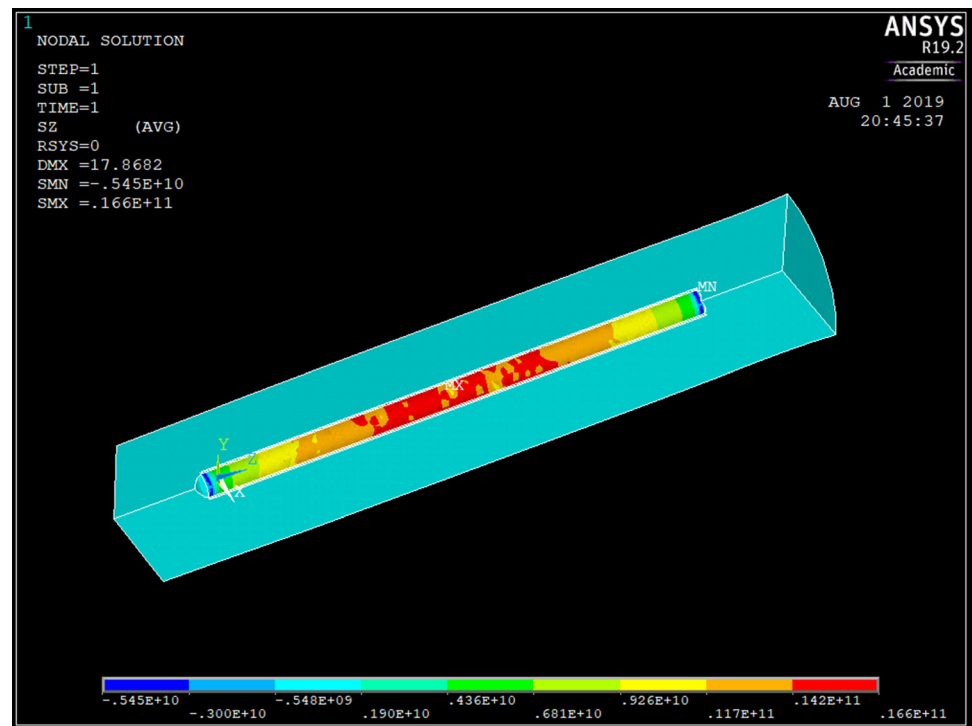
Fig. 22 The FEM elastic modulus for HDPE/SWCNT nanocomposites at a specified weight fraction of SWCNT for both processing techniques

Fig. 23 Comparison of the numerical FEM with the experimental average elastic modulus results of HDPE/SWCNTs nanocomposites processed according to injection moulding

5 Conclusions

In this work, the HDPE matrix was reinforced with SWCNTs nanoparticles. Various combinations of HDPE with 0 wt%, 0.2 wt%, 0.4 wt%, 0.6 wt%, 0.8 wt%, and 1 wt% weight fractions of SWCNTs were prepared through the melting method with twin screw extruder. Then using injection and compression moulding devices, different HDPE/SWCNTs tensile test samples were prepared. In the next phase, tensile tests and numerical FEM predictions of the HDPE/SWCNTs nanocomposites elastic modulus were performed and eventually, the following results were obtained:

- The tensile test showed that elastic modulus, yield stress, and the maximum force of HDPE were improved through the addition of the SWCNTs nanoparticles weight fractions.
- The tensile result also showed that injection moulding yield HDPE/SWCNTs nanocomposites with improved elastic modulus compared to compression moulding.
- Signal to noise ratio results confirmed that addition of SWCNTs nanoparticles has more effect on the improvement of the elastic modulus of HDPE/SWCNTs nanocomposite, through showing that at 1 wt% SWCNTs the of HDPE/SWCNTs nanocomposites
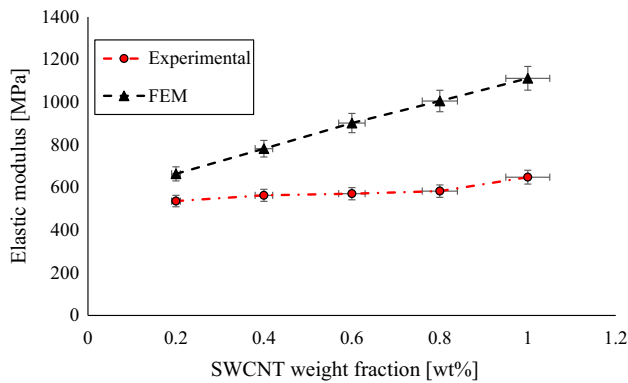
Fig. 24 Comparison of the numerical FEM with the experimental average elastic modulus results of HDPE/SWCNTs nanocomposites processed according to compression moulding

elastic modulus improved by 24% compared to that of two processing.

- The numerical FEM results showed the potentials of predicting the elastic modulus of HDPE/SWCNTs nanocomposites with more accuracy compared to experimentation.

Appendix 1

From Table 5, the average elastic modulus of HDPE (0 wt%) for injection moulding and compression moulding which are 581.198 MPa and 534.855 MPa respectively. Were used to calculate the difference percentage as:

$$\frac{581.198 - 534.855}{534.855} \times 100 \approx 9\% \qquad (12)$$

Again, From Table 5, the average elastic modulus of HDPE/SWCNTs nanocomposite (1 wt%) for injection moulding and compression moulding which are 737.0032 MPa and 648.392 MPa respectively. Were used to calculate the difference percentage as:

$$\frac{737.032 - 648.392}{648.392} \times 100 \approx 14\% \qquad (13)$$

From Table 6, the average amount of elastic modulus of HDPE/SWCNTs nanocomposite at 0 wt% and 1 wt% which are 692.712 MPa and 55.027 MPa respectively were used to calculate the following percentage difference:

$$\frac{692.712 - 558.027}{558.027} \times 100 \approx 24\%. \qquad (14)$$

References

Ahmadi M, Ansari R, Hassanzadeh-Aghdam MK (2019) Micromechanical analysis of elastic modulus of carbon nanotube-aluminium nanocomposites with random microstructures. J Alloys Compd 779:433–439. https://doi.org/10.1016/j.jallcom.2018.11.326

ASTM D638 - 14 Standard Test Method for Tensile Properties of Plastics (n.d.). https://www.astm.org/Standards/D638. Accessed 21 Jan 2020

Azizi S, Fattahi AM, Kahnamouei JT (2015a) Evaluating mechanical properties of nanoplatelet reinforced composites under mechanical and thermal loads. J Comput Theor Nanosci 12:4179–4185. https://doi.org/10.1166/jctn.2015.4334

Azizi S, Safaei B, Fattahi AM, Tekere M (2015b) Nonlinear vibrational analysis of nanobeams embedded in an elastic medium including surface stress effects. Adv Mater Sci Eng. https://doi.org/10.1155/2015/318539

Barai P, Weng GJ (2011) Theory of plasticity for carbon nanotube reinforced composites. Int J Plast 27:539–559. https://doi.org/10.1016/j.ijplas.2010.08.006

Corbridge DM, Harper LT, De Focatiis DSA, Warrior NA (2017) Compression moulding of composites with hybrid fibre architectures. Compos Part A Appl Sci Manuf 95:87–99. https://doi.org/10.1016/j.compositesa.2016.12.018

Crawford RJ (1998) Plastics engineering. Elsevier. https://doi.org/10.1016/b978-0-7506-3764-0.x5000-6

De Roover B, Sclavons M, Carlier V, Devaux J, Legras R, Momtaz A (1995) Molecular characterization of maleic anhydride-functionalized polypropylene. J Polym Sci, Part A: Polym Chem 33:829–842. https://doi.org/10.1002/pola.1995.080330509

Dehghani H, Brooksby B, Vishwanath K, Pogue BW, Paulsen KD (2003) The effects of internal refractive index variation in near-infrared optical tomography: a finite element modelling approach. Phys Med Biol 48:2713–2727. https://doi.org/10.1088/0031-9155/48/16/310

Fattahi AM, Safaei B (2017) Buckling analysis of CNT-reinforced beams with arbitrary boundary conditions. Microsyst Technol. https://doi.org/10.1007/s00542-017-3345-5

Fattahi AM, Roozpeikar S, Ahmed NA (2018) FEM modelling based on molecular results for PE/SWCNT nanocomposites. Int J Eng Technol 7:4345–4356. https://doi.org/10.14419/ijet.v7i4.10498

Fattahi AM, Safaei B, Ahmed NA (2019a) A comparison for the non-classical plate model based on axial buckling of single-layered graphene sheets. Eur Phys J Plus. https://doi.org/10.1140/epjp/i2019-12912-7

Fattahi AM, Safaei B, Moaddab E (2019b) The application of nonlocal elasticity to determine vibrational behavior of FG nanoplates. Steel Compos Struct. https://doi.org/10.12989/scs.2019.32.2.281

Galgali G, Agarwal S, Lele A (2004) Effect of clay orientation on the tensile modulus of polypropylene-nanoclay composites. Polymer (Guildf) 45:6059–6069. https://doi.org/10.1016/j.polymer.2004.06.027

Griebel M, Hamaekers J (2004) Molecular dynamics simulations of the elastic moduli of polymer-carbon nanotube composites. Comput Methods Appl Mech Eng 193:1773–1788. https://doi.org/10.1016/j.cma.2003.12.025

Hasegawa N, Kawasumi M, Kato M, Usuki A, Okada A (1998) Preparation and mechanical properties of polypropylene-clay hybrids using a maleic anhydride-modified polypropylene oligomer. J Appl Polym Sci 67:87–92. https://doi.org/10.1002/(SICI)1097-4628(19980103)67:1%3c87:AID-APP10%3e3.0.CO;2-2

Hassanzadeh-Aghdam MK, Ansari R, Darvizeh A (2018) Micromechanical analysis of carbon nanotube-coated fibre-reinforced hybrid composites. Int J Eng Sci 130:215–229. https://doi.org/10.1016/j.ijengsci.2018.06.001

Ho MP, Wang H, Lee JH, Ho CK, Lau KT, Leng J et al (2012) Critical factors on manufacturing processes of natural fibre composites. Compos Part B Eng 43:3549–3562. https://doi.org/10.1016/j.compositesb.2011.10.001

Hoffman JD, Frankel S (2018) Numerical methods for engineers and scientists. CRC press

Horritt MS, Bates PD (2001) Predicting floodplain inundation: raster-based modelling versus the finite-element approach. Hydrol Process Hydrol Process 15:825–842. https://doi.org/10.1002/hyp.188

Huang ZM, Zhang YZ, Kotaki M, Ramakrishna S (2003) A review on polymer nanofibers by electrospinning and their applications in nanocomposites. Compos Sci Technol 63:2223–2253. https://doi.org/10.1016/S0266-3538(03)00178-7

Huang R, Xu X, Lee S, Zhang Y, Kim BJ, Wu Q (2013) High-density polyethylene composites reinforced with hybrid inorganic fillers: morphology, mechanical and thermal expansion performance. Materials 6(9):4122–4138

ISO—ISO 527-1:2012 (n.d.) Plastics—determination of tensile properties: part 1: general principles. https://www.iso.org/standard/56045.html. Accessed 21 Jan 2020

Jahan SA, El-Mounayri H (2016) Optimal conformal cooling channels in 3D printed dies for plastic injection molding. Procedia Manuf 5:888–900. https://doi.org/10.1016/j.promfg.2016.08.076

Jalali MH, Shahriari B, Zargar O, Baghani M, Baniassadi M (2018) Free vibration analysis of rotating functionally graded annular disc of variable thickness using generalized differential quadrature method. Sci Iran 25(2):728–740

Jalali MH, Zargar O, Baghani M (2019) Size-dependent vibration analysis of FG microbeams in a thermal environment based on modified couple stress theory. Iran J Sci Technol Trans Mech Eng 43(1):761–771

Joshi P, Upadhyay SH (2014) Evaluation of elastic properties of multi-walled carbon nanotube-reinforced composites. Comput Mater Sci 81:332–338. https://doi.org/10.1016/j.commatsci.2013.08.034

Kanit T, Forest S, Galliet I, Mounoury V, Jeulin D (2003) Determination of the size of the representative volume element for random composites: statistical and numerical approach. Int J Solids Struct 40:3647–3679. https://doi.org/10.1016/S0020-7683(03)00143-4

Kwon YI, Lim E, Song YS (2018) Simulation of injection-compression moulding for thin and large battery housing. Curr Appl Phys 18:1451–1457. https://doi.org/10.1016/j.cap.2018.08.017

Liu T, Wang A, Wang Q, Qin B (2020) Wave based method for free vibration characteristics of functionally graded cylindrical shells with arbitrary boundary conditions. Thin-Walled Struct. https://doi.org/10.1016/j.tws.2019.106580

MatWeb LL (2013) MatWeb, your source for materials information. MatWeb Material Property Data. (1996–2007), Automation Creations, Inc

Moaveni S (2003) Finite element analysis—theory and applications with ANSYS, 2nd edn. Pearson Education, Upper Saddle River. ISBN 0-13-111202-3

Mohammadsalehi M, Zargar O, Baghani M (2017) Study of non-uniform viscoelastic nanoplates vibration based on nonlocal first-order shear deformation theory. Meccanica 52(4–5):1063–1077

Najipour A, Fattahi AM (2017) Experimental study on mechanical properties of PE/CNT composites. J Theor Appl Mech 55:719–726. https://doi.org/10.15632/jtam-pl.55.2.719

Namilae S, Chandra N (2005) Multiscale model to study the effect of interfaces in carbon nanotube-based composites. J Eng Mater Technol Trans ASME 127:222–232. https://doi.org/10.1115/1.1857940

Ngabonziza Y, Li J, Barry CF (2011) Electrical conductivity and mechanical properties of multiwalled carbon nanotube-reinforced polypropylene nanocomposites. Acta Mech 220:289–298. https://doi.org/10.1007/s00707-011-0486-y

Park HS, Phuong DX, Kumar S (2019) AI based injection molding process for consistent product quality. Procedia Manuf. https://doi.org/10.1016/j.promfg.2018.12.017

Qian D, Dickey EC, Andrews R, Rantell T (2000) Load transfer and deformation mechanisms in carbon nanotube-polystyrene composites. Appl Phys Lett 76:2868–2870. https://doi.org/10.1063/1.126500

Qin Z, Chu F, Zu J (2017) Free vibrations of cylindrical shells with arbitrary boundary conditions: a comparison study. Int J Mech Sci 133:91–99. https://doi.org/10.1016/j.ijmecsci.2017.08.012

Qin Z, Pang X, Safaei B, Chu F (2019a) Free vibration analysis of rotating functionally graded CNT reinforced composite cylindrical shells with arbitrary boundary conditions. Compos Struct. https://doi.org/10.1016/j.compstruct.2019.04.046

Qin Z, Safaei B, Pang X, Chu F (2019b) Traveling wave analysis of rotating functionally graded graphene platelet reinforced nanocomposite cylindrical shells with general boundary conditions. Results Phys. https://doi.org/10.1016/j.rinp.2019.102752

Qin Z, Zhao S, Pang X, Safaei B, Chu F (2020a) A unified solution for vibration analysis of laminated functionally graded shallow shells reinforced by graphene with general boundary conditions. Int J Mech Sci. https://doi.org/10.1016/j.ijmecsci.2019.105341

Qin B, Zhong R, Wang T, Wang Q, Xu Y, Hu Z (2020b) A unified Fourier series solution for vibration analysis of FG-CNTRC cylindrical, conical shells and annular plates with arbitrary boundary conditions. Compos Struct. https://doi.org/10.1016/j.compstruct.2019.111549

Safaei B, Fattahi AM (2017) Free vibrational response of single-layered graphene sheets embedded in an elastic matrix using different nonlocal plate models. Mechanika. https://doi.org/10.5755/j01.mech.23.5.14883

Safaei M, Sheidaei A, Baniassadi M, Ahzi S, Mosavi Mashhadi M, Pourboghrat F (2015) An interfacial debonding-induced damage model for graphite nanoplatelet polymer composites. Comput Mater Sci 96:191–199. https://doi.org/10.1016/j.commatsci.2014.08.036

Safaei B, Fattahi AM, Chu F (2018) Finite element study on elastic transition in platelet reinforced composites. Microsyst Technol. https://doi.org/10.1007/s00542-017-3651-y

Safaei B, Moradi-Dastjerdi R, Qin Z, Behdinan K, Chu F (2019a) Determination of thermoelastic stress wave propagation in nanocomposite sandwich plates reinforced by clusters of carbon nanotubes. J Sandw Struct Mater. https://doi.org/10.1177/1099636219848282

Safaei B, Ahmed NA, Fattahi AM (2019b) Free vibration analysis of polyethylene/CNT plates. Eur Phys J Plus. https://doi.org/10.1140/epjp/i2019-12650-x

Safaei B, Moradi-Dastjerdi R, Behdinan K, Qin Z, Chu F (2019c) Thermoelastic behavior of sandwich plates with porous polymeric core and CNT clusters/polymer nanocomposite layers. Compos Struct. https://doi.org/10.1016/j.compstruct.2019.111209

Sharma SK, Nayak SK (2009) Surface modified clay/polypropylene (PP) nanocomposites: effect on physico-mechanical, thermal and morphological properties. Polym Degrad Stab 94:132–138. https://doi.org/10.1016/j.polymdegradstab.2008.09.004

Tebeta RT, Fattahi AM, Ahmed NA (2019) Prediction of the elastic behaviour of HDPE/SWCNTs nanocomposites with FEM approach. In: Journal of physics: conference series, vol 1378. Institute of Physics Publishing. https://doi.org/10.1088/1742-6596/1378/3/032073

Thakur SK, Sharma A, Batra NK (2012) Tribological characterization of CNT/HDPE polymer nano-composites. Int J Theor Appl Res Mech Eng 1:32–36

Thomas B, Roy T (2016) Vibration analysis of functionally graded carbon nanotube-reinforced composite shell structures. Acta Mech 227:581–599. https://doi.org/10.1007/s00707-015-1479-z

Ullah Z (2012) Nanotechnology and its impact on modern computer. Glob J Res Eng 12:4

Wang T-Y, Liu S-C, Tsai J-L (2016) Micromechanical stick-slip model for characterizing damping responses of single-walled carbon nanotube nanocomposites. J Compos Mater 50:57–73. https://doi.org/10.1177/0021998315570371

Wu CL, Zhang MQ, Rong MZ, Friedrich K (2002) Tensile performance improvement of low nanoparticles filled-polypropylene composites. Compos Sci Technol 62:1327–1340. https://doi.org/10.1016/S0266-3538(02)00079-9

Yang X, Sahmani S, Safaei B (2020) Postbuckling analysis of hydrostatic pressurized FGM microsized shells including strain gradient and stress-driven nonlocal effects. Eng Comput. https://doi.org/10.1007/s00366-019-00901-2